PCCP

Accepted Manuscript

ROYAL SOCIETY OF CHEMISTRY

www.rsc.org/pccp

Journal Name

RSCPublishing

COMMUNICATION

Cracked polymer templated metal network as transparent conducting electrode for ITO-free organic solar cells

Cite this: DOI: 10.1039/x0xx00000x

Received 00th January 2012,
Accepted 00th January 2012

DOI: 10.1039/x0xx00000x

www.rsc.org/

K.D.M. Rao[1], Christoph Hunger[2], Ritu Gupta[1], Giridhar U. Kulkarni[1,*], Mukundan Thelakkat[2,*]

We report a highly transparent, low resistant Ag metal network templated from a cracked polymer thin film and its incorporation in an organic solar cell. The performance of this scalable metallic network is comparable to that of conventional ITO electrode. This is a general approach to replace ITO in diverse thin film devices.

Organic solar cells (OSCs) are an attractive option for large area and inexpensive production of modules. This is because OSCs are well suited to low cost manufacturing due to simple processing[1] steps that are easily translated to roll-to-roll mass production[2] and leading to near commercialization. In the recent past, extensive research has been carried out on the active semiconductor ingredients[3] and electrode optimization[4] in order to improve the OSC performance,[5] which is typically poorer compared to other types of solar cells such as dye sensitized solar cells[6] and silicon based solar cells.[7, 8] Nonetheless, OSCs occupy unique position in photovoltaic roadmap as solid state, flexible, environmentally benign and ultralight large area devices.[9]

In OSCs, indium tin oxide (ITO) is the most commonly used transparent conducting electrode. Best ITO films exhibit transmittance of 92% in the visible region and a sheet resistance of 10 ohm/□.[10] Indium is scarce and expensive;[11] ITO requires high temperature processing and is brittle, develops cracks on flexible substrates.[12] In order to address these issues, there has been much effort in the literature towards alternative electrodes. Graphene,[13] carbon nanotubes (CNT),[14, 15] and Ag nanowires[16, 17] have been proposed as alternatives to ITO. Graphene has outstanding optical properties, but limited sheet resistance of 30 ohm/□.[13] The CNT networks also exhibit high sheet resistance and in addition, are less stable in the ambient.[14, 18] Ag nanowire networks show relatively superior performance in terms of transmittance and sheet resistance.[17] but like any networks produced from pre-synthesized nanowires (tubes), they suffer from contact resistance at innumerable crossbar junctions and high roughness.[19, 20] Further, the redundant wire/tubes in the network can short the OSCs, which restricted its use in roll-to-roll fabrication. Often, they require an extra treatment to improve the performance, such as mechanical pressing,[21] thermal treatment[20] or poly(3,4-ethylenedioxythiophene) poly(styrenesulfonate) (PEDOT:PSS) coating.[19]

Metal grids offer attractive alternatives to the above TCEs.[22-30] Indeed being free of junctions, they exhibit high performance in terms of transmittance and sheet resistance, and have been successfully used in optoelectronic devices including OSCs. Typically, they are produced by patterning using lithographic techniques such as photolithography,[22] soft lithography,[23] phase shift lithography[24] and nanoimprint lithography.[25] A technologically relevant and simple alternative is the direct printing of grids from silver nanoparticle inks either by ink-jet printing[26,27] or laser printing [27,28] or flexographic and thermal imprinting[30].These recipes for Ag grids result in relatively large feature sizes. Such printed patterns are often used as current collecting grids in diverse applications.

Recently, metal meshes have been fabricated based on cracked TiO2 templates and their application for such fabricated metal meshes in touchscreens were shown.[31,32] Some of us[33] have shown very recently selective deposition of Cu by electroplating in the cracked regions of a polymer template to produce Cu mesh based TCE. These cracked template methods are highly scalable but need to be tested for their applicability and device integration in thin film organic devices such as OSC, OFET etc. One of the basic challenges is to obtain high light transmission maintaining low sheet resistance for such TCEs. Additionally, in thin film devices, the uniformity and connectivity of such meshes are very critical for the reproducibility of such devices.

In this article, we have explored the feasibility of cracking as a tool for the preparation of such metal meshes from inexpensive polymer templates at room temperature and integrating them as TCEs in bulk heterojunction OSCs. Specifically, using seamless Ag network in the form of a mesh as a replacement for ITO electrodes, several OSCs have been made in inverted geometry, which exhibited performance comparable to those produced with ITO. We like to note that this work emphasizes the suitability and reproducibility of such an ITO-free TCE in OSC and not specifically the optimization of efficiency of any kind of device.

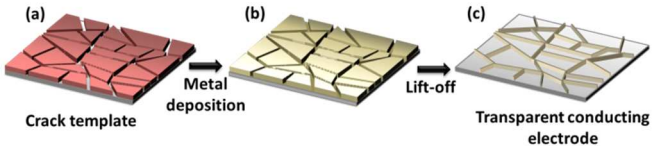

Fig. 1 Schematic illustration of transparent conducting electrode fabrication (a) Cracked template (b) deposition of metal on cracked template and (c) lift-off of the template giving rise to Ag network based TCE.

The process flow for templating is shown schematically in Fig. 1. First, a crack layer is produced by drying an acrylic based colloidal dispersion on glass substrate wherein highly interconnected cracks are spontaneously obtained. These are U-shaped grooves are complete cracks down to the substrate to be distinguished from incomplete cracks.[34] Using the cracked template, metal (Ag, 55 nm) is deposited by vacuum evaporation and subsequently, the template is washed away in chloroform.

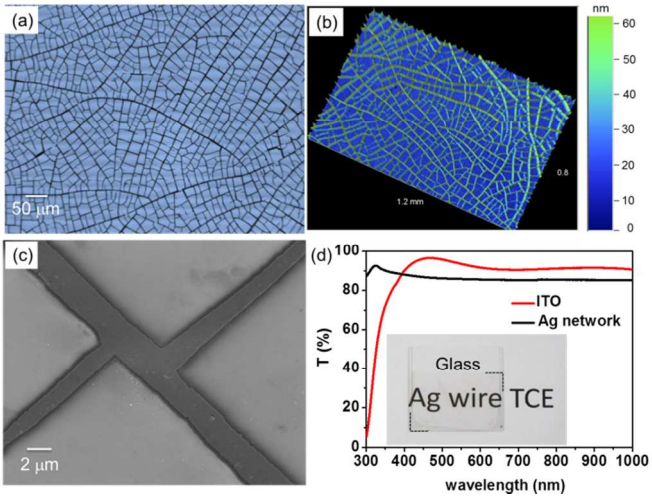

Fig. 2 Characterization of Ag network derived TCE: (a) Optical microscope image (transmission mode), (b) optical profiler image in 3D view, (c) SEM image of a network junction and (d) comparison of transmittance spectra of Ag metallic network and ITO. Inset shows the photograph of Ag network TCE on glass substrate.

As shown in Fig. 2a, the Ag mesostructures on glass appear well interconnected throughout the network. The metal fill factor is estimated to be ~ 20% with structural width of ~ 2 μm and average cell size (spacing between the Ag structures) of 20 to 60 μm. The optical profilometric image (1.2 x 0.8 mm^2) in Fig. 2b not only reveals the connectivity of the Ag network over large area but also shows its seamless nature. The surface roughness of the network is estimated to be ~ 5 nm while the peak to valley roughness, which corresponds to network thickness, is 55 nm. The SEM image in Fig. 2c shows a junction where the network surface continues to be smooth and the junction itself is seamless unlike crossbar junctions commonly seen in network TCEs made from pre-synthesized Ag nanowires.[21] Accordingly, the sheet resistance was found to be ~ 10 ohm/□, which is rather low considering the thickness of only 55 nm. The transmittance of Ag network was ~ 86% at 550 nm (see Fig. 2d) and the overall transmittance is comparable to that exhibited by ITO but importantly, extends down to UV region (see photograph in the inset). ITO, on the other hand, is a good UV absorber.

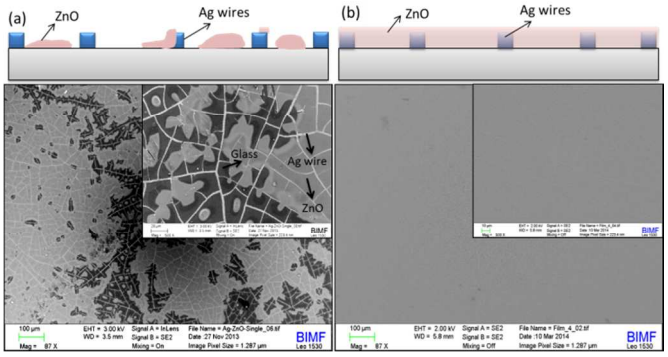

Fig. 3: SEM images and schematic illustrations of Ag network TCE covered with ZnO for layer thickness of (a) 45 nm and (b) 135 nm. For more SEM images, see supporting information, Fig. S1.

In the next step of solar cell fabrication, ZnO barrier layer was brought in by decomposing zinc acetate film at 150 °C in air (see supporting information for experimental details).[35] For a proposed thickness of 45 nm of ZnO, the obtained layer was non-uniform and discontinuous (Fig. 3a) as evident from the dark and grey regions, the latter corresponding to ZnO covered network. Beiley et al. described previously the fabrication of a Ag nanowire-ZnO nanoparticle composite to obtain semi-transparent top electrode and achieved a good power conversion efficiency of 4.3% in PBDTTPD/PC_{70}BM devices.[36] Based on this fact, we increased the thickness of the ZnO layer to 95 nm , 135 nm and 230 nm. We observed increasing degree of covering of the metal network with increasing thickness of ZnO. For example, in the SEM image of 135 nm ZnO layer shown in Fig. 3b, the ZnO film is seen to be uniformly submerging the entire Ag network. This is found to be the optimal ZnO thickness required to submerge the 55 nm thick Ag network so as to have reproducible devices without shorting.

Four bottom-illuminated inverted photovoltaic cells (5 devices in each) consisting of poly-3-hexylthiophene (P3HT) and phenyl-C61-butyric acid methyl ester (PCBM) were fabricated on a glass substrate as shown in the schematic in Fig. 4a with Ag network derived TCE. The bar graphs of solar cell parameters (Voc, Jsc, FF and □) for all the four cells with varying thicknesses of ZnO barrier layer are shown in Fig. 4b. In cell 1, all five devices with 45 nm of ZnO layer were defective due to shorting. For cell 2 with 95 nm ZnO layer, only two devices were working with moderate efficiencies. On the other hand, for cells 3 and 4 with 135 and 230 nm ZnO barrier layer thicknesses respectively, all five devices were found to be functioning. Significantly, with 135 nm ZnO (cell 3), the five devices showed uniform performance with average efficiency of 2.26 ± 0.05% while those from 230 nm ZnO, exhibited some variation in performance with lower efficiency (1.34 ± 0.43%, see Fig. 4b).

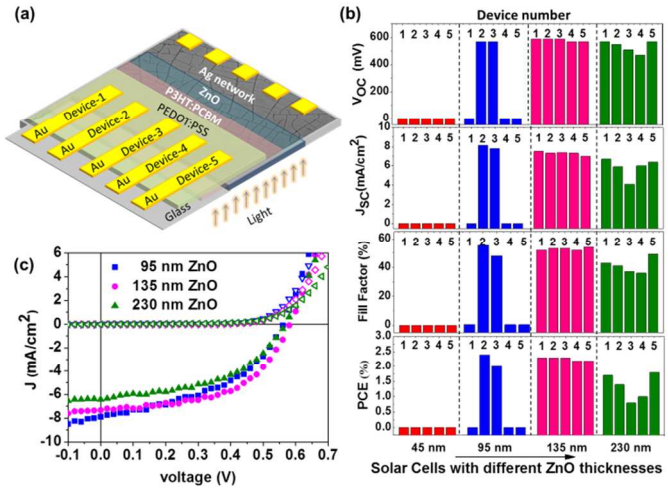

Fig. 4 (a) Schematic illustration of the inverted P3HT-PCBM solar cell with Ag network TCE, (b) bar graph of cell parameters for solar cells of different ZnO layer thicknesses (45, 95, 135 and 230 nm), (c) examples of J-V characteristics of solar cells with different ZnO layer thicknesses in dark (open symbols) and in light (filled symbols). Note that best performing solar cell is chosen from each cell.

The decrease in the cell efficiency for higher ZnO thicknesses can be attributed to higher series resistance of the cell leading to lower current density and fill factor values (see Fig. 4b).[35] Indeed, the variations in solar cell parameters among the five devices exhibit similar trend. The J-V characteristics of typical solar cells with different ZnO layer thicknesses (95 nm, 135 nm, 230 nm) are shown in Fig. 4b (see supporting information Fig. S2 for J-V characteristics of all working devices).

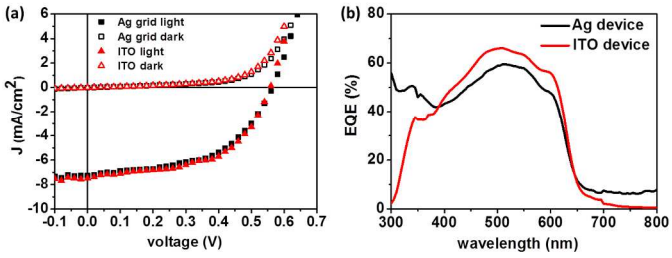

Fig. 5 Comparison of (a) J-V characteristics and (b) EQE for optimized Ag network and ITO devices.

In Fig. 5a, we compare the J-V characteristics of a typical device fabricated using Ag network (from cell 3) with that produced using ITO as TCE (ITO: T= 93% and Rs= 16 ohm/□). The Ag network cell has an optimum thickness of 135 nm of ZnO. For ITO device, the thickness of ZnO blocking layer was kept at 45 nm which is optimum for an inverted solar cell.[35] All other process parameters such as active layer thickness, top electrode, annealing temperature etc. were kept the same for all the devices. It is clear from the plot that the Ag network TCE based solar cell follows a similar trend as the ITO based cell and the derived parameters are quite comparable (see Table 1). Thus, the efficiency of Ag network TCE based solar cell was 2.14%, while that obtained for ITO based cell under similar conditions in ambient was 2.27%.

TCE	Voc (v)	Jsc (mA/cm^2)	FF (%)	N (%)	Rsh Ω/ cm^2	Rs Ω/ cm^2 @Voc	Rs Ω/ cm^2 @Pmax
Ag grid	0.57	7.2	51.8	2.14	421	8.3	49.7
ITO	0.55	7.5	55.2	2.27	413	6.7	48.6

Table 1 Summary of the solar cell parameters corresponding to J-V characteristics shown in Figure 5a. Note, that Ag grid device has a 135 nm thick ZnO layer, whereas ITO device has a ZnO layer of only 45 nm.

These results presented here clearly demonstrate the potential of Ag network based TCE as an alternative to ITO in OSCs. However, a slightly thicker ZnO layer is required to cover the Ag network thickness. Since the ZnO is filled in the interstitial domains between the metallic network, it improves the charge collection properties, which is similar to coating a PEDOT:PSS layer as reported for conventional metal grids.[19] The external quantum efficiency (EQE) measurements (Fig. 5b) show that the Ag network TCE based cell exhibits slightly less values in the visible region compared to those derived from ITO cell, but in the UV region, the former excels which makes the overall performance similar for both cells. This can be clearly understood from the differences in transmission of the respective electrodes in the UV region (Fig. 2d). The same information can be inferred on comparing the absorption spectra of the two solar cells (supporting information Fig. S3) with their EQE spectra.

The method developed in this study for TCE and associated OSC fabrication has several merits. While the present study has focused on only one type of metallic network, its scope of application can be easily extended to other thin layer devices by varying the template thickness and other parameters in the initial stages of crack template formation. Thus, it is possible to obtain TCEs with different network thicknesses and connectivity and importantly with different metals. Here, Ag was used as a typical example since the work function is favorable for inverted geometry P3HT-PCBM solar cell. However, it can be replaced with other metals such as Cu, Al, Pt depending on the need of application. The metal network based TCE used in the present study works as current collecting grid at tens of micrometer scale with a metal fill factor of 20%.

Conclusions

In conclusion, we demonstrated the incorporation of a highly transparent and highly conducting Ag metallic network obtained using a cracked polymer template, in a thin film organic solar cell for the first time. The performance of this highly scalable metal network as a TCE is comparable to that of conventional ITO electrode. This is a general approach to replace ITO in diverse thin film devices. The crack template approach is universal for any type of metal or substrate material.

Acknowledgements

The financial support from EU Project "Largecells" (Grant No. 261936), Department of Science and Technology, Government of India, and Bavarian State Ministry of Science, Research, and Arts for the collaborative Research Network "Solar Technologies go Hybrid" is gratefully acknowledged. G.U.K., R.G. and K.D.M.R. are grateful to Professor C. N. R. Rao for his encouragement. K.D.M.R.

thanks UGC for the SRF fellowship and C. H. acknowledges financial support from DFG (GRK 1640).

Notes and references

[1] Chemistry & Physics of Materials Unit and Thematic Unit of Excellence in Nanochemistry, Jawaharlal Nehru Centre for Advanced Scientific Research, Jakkur P.O., Bangalore 560 064, India.
[2] Applied Functional Polymers, Macromolecular Chemistry I, University of Bayreuth, D-95440 Bayreuth, Germany.
*E-mail: kulkarni@jncasr.ac.in; mukundan.thelakkat@uni-bayreuth.de

† Electronic Supplementary Information (ESI) available: Experimental details of device preparation, additional SEM and J/V curves of devices. See DOI: 10.1039/c000000x/

1 Y. Sun, G. C. Welch, W. L. Leong, C. J. Takacs, G. C. Bazan and A. J. Heeger, *Nat. Mater* 2012, **11**, 44.
2 a) F. C. Krebs, *Sol. Energy Mater. Sol. Cells* 2009, **93**, 465; b) R. Gupta, S. Kiruthika, K. D. M. Rao, M. Jørgensen, F. C. Krebs and G. U. Kulkarni, *Energy Technol.* 2013, **1**, 770; c) D. Angmo, S. A. Gevorgyan, T. T. Larsen-Olsen, R. R. Søndergaard, M. Hösel, M. Jørgensen, R. Gupta, G. U. Kulkarni and F. C. Krebs, *Org. Electron.* 2013, **14**, 984.
3 L. Bian, E. Zhu, J. Tang, W. Tang and F. Zhang, *Prog. Polym. Sci.* 2012, **37**, 1292.
4 Y. H. Kim, C. Sachse, M. L. Machala, C. May, L. Müller-Meskamp and K. Leo, *Adv. Funct. Mater.* 2011, **21**, 1076.
5 T. Ameri, N. Li and C. J. Brabec, *Energy Environ. Sci.* 2013, **6**, 2390.
6 A. Hagfeldt, G. Boschloo, L. Sun, L. Kloo and H. Pettersson, *Chem. Rev.* 2010, **110**, 6595.
7 M. A. Green, K. Emery, Y. Hishikawa, W. Warta and E. D. Dunlop, *Prog. Photovoltaics* 2012, **20**, 12.
8 J. Yoo, G. Yu and J. Yi, *Sol. Energy Mater. Sol. Cells* 2011, **95**, 2.
9 M. Kaltenbrunner, M. S. White, E. D. Głowacki, T. Sekitani, T. Someya, N. S. Sariciftci and S. Bauer, *Nat. Commun.* 2012, **3**, 770.
10 H. Kim, C. M. Gilmore, A. Pique, J. S. Horwitz, H. Mattoussi, H. Murata, Z. H. Kafafi and D. B. Chrisey, *J. Appl. Phys.* 1999, **86**, 6451.
11 A. Kumar and C. Zhou, *ACS Nano* 2010, **4**, 11.
12 D. R. Cairns, R. P. Witte, D. K. Sparacin, S. M. Sachsman, D. C. Paine, G. P. Crawford and R. R. Newton, *Appl. Phys. Lett.* 2000, **76**, 1425.
13 S. Bae, H. Kim, Y. Lee, X. Xu, J. S. Park, Y. Zheng, J. Balakrishnan, T. Lei, H. Ri Kim, Y. I. Song, Y. J. Kim, K. S. Kim, B. Ozyilmaz, J.-H. Ahn, B. H. Hong and S. Iijima, *Nat. Nanotechnol.* 2010, **5**, 574.
14 R. C. Tenent, T. M. Barnes, J. D. Bergeson, A. J. Ferguson, B. To, L. M. Gedvilas, M. J. Heben and J. L. Blackburn, *Adv. Mater.*, 2009, **21**, 3210.
15 H. Z. Geng, K. K. Kim, K. P. So, Y. S. Lee, Y. Chang and Y. H. Lee, *J. Am. Chem. Soc.* 2007, **129**, 7758.
16 S. De, T. M. Higgins, P. E. Lyons, E. M. Doherty, P. N. Nirmalraj, W. J. Blau, J. J. Boland and J. N. Coleman, *ACS Nano* 2009, **3**, 1767.
17 D. Kim, L. Zhu, D. J. Jeong, K. Chun, Y. Y. Bang, S. R. Kim, J. H. Kim and S. K. Oh, *Carbon* 2013, **63**, 530.
18 D. Zhang, K. Ryu, X. Liu, E. Polikarpov, J. Ly, M. E. Tompson and C. Zhou, *Nano Lett.* 2006, **6**, 1880.
19 W. Gaynor, G. F. Burkhard, M. D. McGehee and P. Peumans, *Adv. Mater.* 2011, **23**, 2905.
20 C. Sahin, A. Elif Selen and U. Husnu Emrah, *Nanotechnology*, 2013, **24**, 125202.
21 L. Hu, H. S. Kim, J. Y. Lee and P. Peumans, Y. Cui, *ACS Nano* 2010, **4**, 2955.
22 a) J. Zou, H. L. Yip, S. K. Hau, A. K. Y. Jen, Appl. Phys. Lett. 2010, 96, 203301; b) D. S. Ghosh, T. L. Chen and V. Pruneri, *Appl. Phys. Lett.* 2010, **96**, 041109.
23 R. Gupta and G. U. Kulkarni, *ACS Appl. Mater. Interfaces*, 2013, **5**, 730.
24 K. Moon Kyu, G. O. Jong, L. Jae Yong and L. J. Guo, *Nanotechnology* 2012, **23**, 344008.
25 M. G. Kang and L. J. Guo, *Adv. Mater.* 2007, **19**, 1391.
26 Y. Galagan, J.-E. J. M. Rubingh, R. Andriessen, C.-C. Fan, P. W. M. Blom, S. C. Veenstra and J. M. Kroon, *Sol. Energ. Mat. Sol. Cells*, 2011, **95**, 1339.
27 Y. Galagan, B. Zimmermann, E. W. C. Coenen, M. Jørgensen, D. M. Tanenbaum, F. C. Krebs, H. Gorter, S. Sabik, L. H. Slooff, S. C. Veenstra, J. M. Kroon and R. Andriessen, *Adv. Energy Mater.,* 2012, **2**, 103.
28 R. Gupta, M. Hösel, J. Jensen, F. C. Krebs and G. U. Kulkarni, *J. Mater. Chem. C* 2014, **2**, 2112-2117.
29 R. Gupta, S. Walia, M. Hösel, J. Jensen, D. Angmo, F. C. Krebs and G. U. Kulkarni, *J. Mater. Chem. A* DOI: 10.1039/C4TA00301B
30 J. S. Yu, I. Kim, J. S. Kim, J. Jo, T. T. L. Olsen, R. R. Søndergaard, M. Hösel, D. Angmo, M. Jørgensen and F. C. Krebs, *Nanoscale* 2012, **4**, 6032.
31 B. Han, K. Pei, Y. Huang, X. Zhang, Q. Rong, Q. Lin, Y. Guo, T. Sun, C. Guo, D. Carnahan, M. Giersig, Y. Wang, J. Gao and Z. Ren, K. Kempa, *Adv. Mater.* 2014, **26**, 873.
32 S. Kiruthika, K. D. M. Rao, A. Kumar, R. Gupta and G. U. Kulkarni, *Mater. Res. Express*, 2014, **1**, 026301.
33 S. Kiruthika, R. Gupta, K. D. M. Rao, S. Chakraborthy, N. Padmavathy and G. U. Kulkarni, *J. Mater. Chem. C*. 2014, **2**, 2089.
34 (a) J. C. Li, X. Gong, D. Wang and D. C. Ba, *Applied Physics A*, 2013, **111**, 645; (b) M. A. Niedermeier, G. Tainter, B. Weiler, P. Lugli, P. Muller-Buschbaum, *J. Mater. Chem. A.* 2013, **1**, 7870.
35 D. Gupta, M. M. Wienk and R. A. J. Janssen, *Adv. Energy Mater.* 2013, **3**, 782.
36 Z. M. Beiley, M. G. Christoforo, P. Gratia, A. R. Bowring, P. Eberspacher, G. Y. Margulis, C. Cabanetos, P. M. Beaujuge, A. Salleo and M. D. McGehee, *Adv. Mater.,* 2013, **25**, 7020.

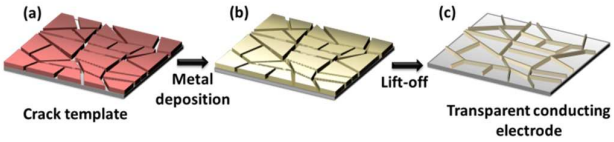

We study the incorporation of a highly transparent and highly conducting Ag metallic network obtained using a cracked polymer template, in a thin film organic solar cell for the first time.